Polarization Switching and Hysteresis in Vertical-Cavity Surface-Emitting Lasers Subject to Orthogonal Optical Injection

Matias F. Salvide, Cristina Masoller, and Maria Susana Torre

***Abstract*— We study polarization switching and hysteresis in a vertical-cavity surface-emitting laser (VCSEL) subject to an orthogonal optical injection, such that the polarization of the injected light is perpendicular to that of the free-running VCSEL. We use the framework of the spin-flip model to characterize the polarization state of the VCSEL as a function of the frequency detuning. With appropriated injection conditions, the orthogonal polarization turns on and locks to the injected field. Increasing and decreasing the detuning across the two locking boundaries results either in narrow or wide hysteresis cycles, or even in irreversible switching. These results are in a good agreement with recent experimental observations.**

***Index Terms*— Vertical-cavity surface-emitting lasers (VCSELs), bistability, polarization switching, optical injection, orthogonal injection.**

I. Introduction

OPTICALLY injected semiconductor lasers display a rich variety of nonlinear phenomena, including stable locking, periodic oscillations, excitable and chaotic behavior [1]–[3]. Regular dynamics can have interesting applications, for example, the period-one oscillation can be used to implement frequency-tunable photonic microwave oscillators [4]–[8]. As vertical-cavity surface-emitting lasers (VCSELs) can emit two orthogonal linear polarization modes, orthogonal optical injection (*i.e.*, injecting light with a polarization that is perpendicular to that of the free-running VCSEL) allows for additional phenomena, such as polarization bistability and switching [9]–[12]. Such polarization bistability and switching can be exploited for implementing all-optical memories [13], logic gates [14], [15], etc.

Here we study polarization switching and hysteresis in a VCSEL subject to orthogonal optical injection from a tunable master laser. The VCSEL dynamics is simulated with the spin-flip model (SFM) [16] that takes into account the coupling between two carrier populations (with spin-up and spin-down) and two optical fields with orthogonal polarizations.

We consider as control parameter the frequency detuning (FD), between the master laser and the free-running slave laser. With strong enough injection, if the detuning is within a range of values, FD2 < FD < FD1, the orthogonal polarization turns on and locks to the injected field. Increasing and decreasing FD across the locking boundaries, either FD1 or FD2, while keeping constant the injected power, results in two successive polarization switchings [17]–[22], one when the injected mode turns on, and one when it turns off. These switchings occur at different values of the detuning when the detuning is increased or is decreased, resulting in hysteresis cycles, which have different features in FD1 and FD2.

Our work is motivated by the recent experimental observation of irreversible polarization switching (IPS) [21] and ultra-wide hysteresis [22]. In [21] the orthogonal mode was observed to persist on even when the control parameter – the injected power or the frequency detuning– was reversed (no switch back was observed). As IPS was observed only in the range of bias currents where two modes are supported (*i.e.*, for $I > 2I_{\rm th}$; for $I < 2I_{\rm th}$ only the fundamental mode is supported and no IPS was observed), IPS was interpreted as a specific feature of the regime of two-mode operation. In [22] the experiments were also performed in the region of two-mode operation, with bias currents above $2I_{\rm th}$, and ultra-wide hysteresis (155 GHz) was observed in the positive detuning region (FD1); in contrast, in the negative detuning region (FD2), the hysteresis cycle had a smaller width (few GHz).

Here we analyze the dependence of the hysteresis width of both cycles on the VCSEL parameters and on the orthogonal optical injection conditions. Regarding the VCSEL parameters, to fit the situation in [21] and [22], they are chosen such that the free-running VCSEL emits a stable linear polarization and no polarization switching occurs over the entire operation range. Regarding the injection conditions, we consider two cases, one in which the free-running laser emits the high-frequency polarization (mode y in the SFM model) and the mode that receives optical injection is the low-frequency polarization (mode x), and one in which the free-running laser emits the low-frequency polarization (mode x) and the injected polarization is the high-frequency one (mode y). We find that, with x-injection (as in [21] and [22]), the width

Manuscript received July 17, 2014; revised August 19, 2014; accepted August 21, 2014. M. F. Salvide and M. S. Torre were supported by the National Scientific and Technical Research Council, Argentina, under Grant PIP 114-200801-00163. C. Masoller was supported in part by the European Office of Aerospace Research and Development under Grant FA8655-12-1-2140, in part by the Spanish Ministerio de Ciencia e Innovacion under Grant FIS2012-37655-C02-01, and in part by the ICREA Academia Programme through the Generalitat de Catalunya under Grant 2009 SGR 1168.

M. F. Salvide and M. S. Torre are with the Facultad de Ciencias Exactas, Instituto de Física Arroyo Seco, Tandil 7000, Argentina (e-mail: marita@exa.unicen.edu.ar; msalvide@exa.unicen.edu.ar).

C. Masoller is with the Departament de Fisica i Enginyeria Nuclear, Universitat Politecnica de Catalunya, Terrassa 08222, Spain (e-mail: cristina.masoller@upc.edu).

Color versions of one or more of the figures in this paper are available online at http://ieeexplore.ieee.org.

Digital Object Identifier 10.1109/JQE.2014.2352032

of the FD1 cycle is much wider than that of the FD2 cycle, and even irreversible PS can be observed, in good agreement with [21] and [22]. On the contrary, our simulations indicate that, with y-injection, the width of the FD2 cycle is wider than that in FD1, and no irreversible PS occurs.

This paper is organized as follows. Section II presents the spin-flip model used for describing the VCSEL dynamics under orthogonal optical injection; Sec. III presents the results of the simulations and Sec. IV presents the discussion of the results and the conclusions.

II. MODEL

We use the well-know spin-flip model of a VCSEL with external optical injection [11]. The equations, written in the frequency reference frame of the injected field are:

$$\frac{dE_x}{dt} = \kappa(1+i\alpha)(NE_x + inE_y - E_x) - i(\gamma_p + \Delta\omega)E_x - \gamma_a E_x + \sqrt{2\beta_{sp}\,\gamma_N N}\ \xi_x + \kappa_x\, E_{inj} \tag{1}$$

$$\frac{dE_y}{dt} = \kappa(1+i\alpha)(NE_y - inE_x - E_y) + i(\gamma_p - \Delta\omega)E_y + \gamma_a E_y + \sqrt{2\beta_{sp}\,\gamma_N N}\ \xi_y + \kappa_y\, E_{inj} \tag{2}$$

$$\frac{dN}{dt} = -\gamma_N\left[N(1+|E_x|^2+\left|E_y\right|^2)\right] + \gamma_N\mu - i\gamma_N n(E_y E_x^* - E_x E_y^*) \tag{3}$$

$$\frac{dn}{dt} = -\gamma_s n - \gamma_N n(|E_x|^2+\left|E_y\right|^2) - i\gamma_N N(E_y E_x^* - E_x E_y^*). \tag{4}$$

Here E_x and E_y are the two orthogonal linearly polarized slowly varying components of the field and N and n are two carrier variables: N accounts for the total carrier density, while n accounts for the difference between two carrier populations (with spin-up and with spin-down). The model parameters are: κ is the field decay rate, γ_N is the decay rate of N, γ_s is the spin-flip relaxation rate, α is the linewidth enhancement factor, γ_a is the linear dichroism (when γ_a is positive the y polarization has the lower threshold), γ_p is the linear birefringence (when γ_p is positive the x polarization has the lower frequency) and μ is the pump current parameter (normalized such that the solitary threshold is at $\mu = 1$ in the absence of anisotropies). Spontaneous emission noise is taken into account by $\xi_x(t)$ and $\xi_y(t)$ that are uncorrelated complex Gaussian noise terms of zero mean. We define the noise strength parameter as $D = 2\gamma_N\ N\ \beta_{sp}$ with β_{sp} being the spontaneous emission factor. We consider parameters well above threshold and approximate $N \approx 1$ since above threshold the N is clamped to the threshold value.

The optical injection parameters are: $E_{inj}, \kappa_x, \kappa_y$, and $\Delta\omega$. E_{inj} is the injected field amplitude; κ_x and κ_y are used to select which polarization receives optical injection:

i) x polarized injection: $\kappa_x = \kappa$ and $\kappa_y = 0$;

ii) y polarized injection: $\kappa_y = \kappa$ and $\kappa_x = 0$.

$\Delta\omega = \omega_{inj} - \omega_{ref}$ is the detuning of the injected field, defined with respect to a reference angular frequency $\omega_{ref} = (\omega_x + \omega_y)/2$, with ω_x and ω_y being the optical angular frequencies of the x and y polarizations: $\omega_x = -\gamma_p + \gamma_a\alpha$, $\omega_y = \gamma_p - \gamma_a\alpha$ [16]. For easy comparison with Refs. [21] and [22],

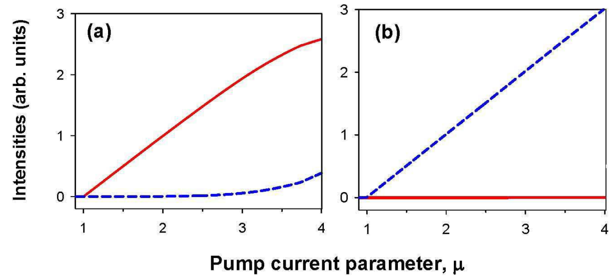

Fig. 1. Polarization-resolved $L-I$ characteristics of the free-running VCSEL. I_{x} (solid, red), I_{y} (dashed, blue). (a) $\gamma_p = 60$ rad/ns, $\gamma_a = -0.1$ ns^{-1} and $\gamma_s = 50$ ns^{-1}; (b) $\gamma_p = 10$ rad/ns, $\gamma_a = 1.5$ ns^{-1} and $\gamma_s = 200$ ns^{-1}; other parameters are as indicated in the text.

we define as control parameter the frequency detuning (FD), which is the difference between the frequency of the injected field and that of the free running VCSEL. Therefore,

i) when the free-running laser emits the y polarization, $\mathrm{FD} = (\omega_{\mathrm{inj}} - \omega_{\mathrm{y}})/2\pi$;

ii) when the free-running laser emits the x polarization, $\mathrm{FD} = (\omega_{\mathrm{inj}} - \omega_{\mathrm{x}})/2\pi$.

Also for easy comparison with [22], the width of the hysteresis cycles are defined as

$$\mathrm{H1} = \mathrm{FD}_4 - \mathrm{FD}_3(\text{high-frequency side})$$
$$\mathrm{H2} = \mathrm{FD}_2 - \mathrm{FD}_{1.}(\text{low-frequency side})$$

where FD_2 and FD_4 (FD_1 and FD_3) are the detuning values for increasing (for decreasing) detuning, when the injected mode turns on and when it turns off.

III. RESULTS

Equations (1)–(4) were simulated with typical VCSEL parameters: $\gamma_N = 1$ ns^{-1}, $\kappa = 300$ ns^{-1}, $\alpha = 3$ and $D = 10^{-5}$ ns^{-1}; for γ_p, γ_a and γ_s we use two sets of values that allow us to consider two situations:

i) For $\gamma_p = 60$ rad/ns, $\gamma_a = -0.1$ ns^{-1} and $\gamma_s = 50$ ns^{-1} the free-running VCSEL emits the lower frequency polarization (x), thus, we consider y polarized optical injection ($\kappa_y = \kappa$, $\kappa_x = 0$).

ii) For $\gamma_p = 10$ rad/ns, $\gamma_a = 1.5$ ns^{-1} and $\gamma_s = 200$ ns^{-1} the free-running VCSEL emits the higher frequency polarization (y), and now the injected light is x polarized ($\kappa_x = \kappa$ and $\kappa_y = 0$). This case corresponds to the VCSELs used in [21] and [22].

For these parameters, as shown in Fig. 1, for the free-running VCSEL no PS occurs for increasing or decreasing pump current (as in [21] and [22]).

A triangular signal was used to increase and decrease the frequency detuning (FD), keeping all other parameters fixed. The total simulation time was long enough to ensure a quasi-static variation of FD (5 μs). The polarization switching points FD_1, FD_2, FD_3 and FD_4 were computed by averaging over 10 stochastic simulations; in each simulation the switching points were detected by averaging the intensities I_{x} and I_{y} over a short time interval (1 ns). The initial conditions were such that the scan of the detuning started from an FD value far (to the left or to the right) from the boundary of the region where the orthogonal polarization turns on.

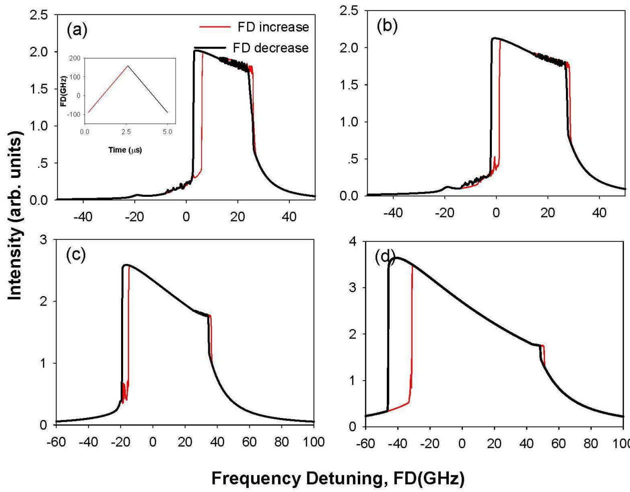

Fig. 2. Polarization behavior under y-injection. For clarity only the intensity of the injected mode (y) is shown, the intensity is averaged over a 1 ns time interval. The frequency detuning, FD, first increases and then decreases, as shown in the inset. $E_{inj} = 0.15$ (a); 0.20 (b); 0.4 (c) and 0.8 (d), $\mu = 2.7$, other parameters are as in Fig. 1a.

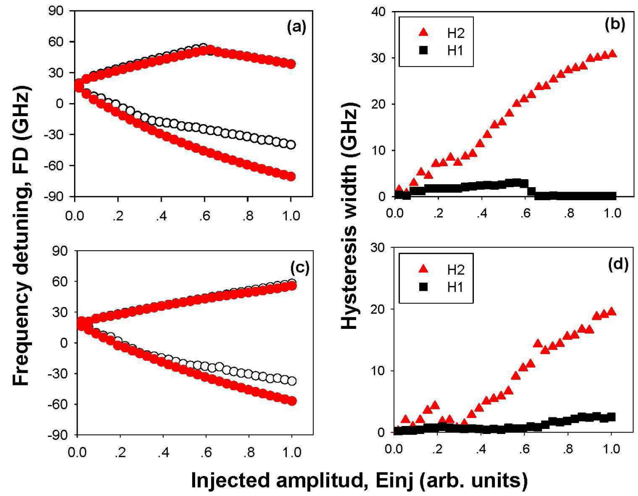

Fig. 3. Polarization switching points when the VCSEL is subjected to y polarized injection (left column, red circles: FD decrease, white circles: FD increase) and width of the hysteresis cycles (right column, H1: black squares, H2: red triangles) vs the amplitude of the injected field, E_{inj}. The pump current parameter is $\mu = 1.8$, (a,b), $\mu = 2.7$ (c, d), other parameters are as Fig 1a.

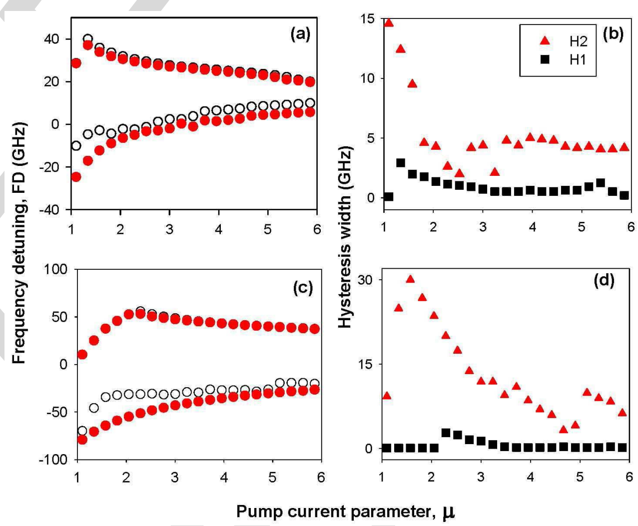

Fig. 4. Polarization switching points when the VCSEL is subjected to y polarized injection (left column, red circles: FD decrease, white circles: FD increase) and width of the hysteresis cycles (right column, H1: black squares, H2: red triangles) vs the bias current parameter, μ. $E_{\mathrm{inj}} = 0.20$ (a,b); 0.8 (c,d); other parameters are as Fig 1a.

Next we present the results of the simulations: first we consider the situation in which the free-running laser emits the x polarization and receives y-polarized injection and then, we consider the situation in which the free-running laser emits the y polarization and receives x-polarized injection.

A. Y Polarized Injection

We consider the first set of parameters, such that the free-running VCSEL emits the x-polarization. We consider orthogonal injection in the y polarization ($\kappa_y = \kappa$, $\kappa_x = 0$). The detuning is defined as $\mathrm{FD} = (\omega_{\mathrm{inj}} - \omega_{\mathrm{x}})/2\pi$.

Figure 2 displays the intensity of the y polarization when the detuning is first increased and then decreased, while the injection strength is kept constant. Simulations for various injection strengths are presented, and it can be observed that the width of the low-frequency side cycle (H2) increases with the injection strength, while the width of the high-frequency side cycle (H1) remains nearly constant.

The left column of Fig. 3 displays the FD values where the y polarization turns on (FD_2 and FD_4) and when it turns off (FD_1 and FD_3) and in the right column, the hysteresis widths (H1 and H2) as a function of the injection strength, for two values of the pump current parameter. With weak optical injection there is polarization competition and the turn-on points of the y polarization are not well defined. This occurs for E_{inj} below 0.05; for stronger injection four switching points define two hysteresis cycles. While the width of the cycle on the high-frequency side, H1, is constant and approximately equal to 3 GHz regardless of the value of E_{inj}, the width of the cycle on the low-frequency side, H2, increases with E_{inj}.

Figure 4 displays the value of the detuning at the four switching points (left column) and the two hysteresis widths (right column) vs the pump current parameter. Simulations for two injection strengths are presented. We observe that for all μ values H1 $<$ H2.

Taken together Figs. 3 and 4 demonstrate that the width of the cycle on the low frequency side (H2) varies with E_{inj} and μ, and large cycles occur for certain parameters ($E_{\mathrm{inj}} \approx 0.8$, $\mu \approx 1.6$). In contrast, the width of the cycle on the high frequency side (H1) is smaller and remains nearly constant when varying E_{inj} or μ.

B. X Polarized Injection

Next we consider the second set of parameters, which correspond to the experimental situation in [21] and [22], such that the free-running laser emits the y polarization and the x polarization receives optical injection ($\kappa_x = \kappa$ and $\kappa_y = 0$). Now the frequency detuning is defined as $\mathrm{FD} = (\omega_{\mathrm{inj}} - \omega_{\mathrm{y}})/2\pi$.

Figure 5 displays intensity of the x polarization when the detuning is varied, while the injection strength is kept constant. Simulations for four injection strengths are presented. For very

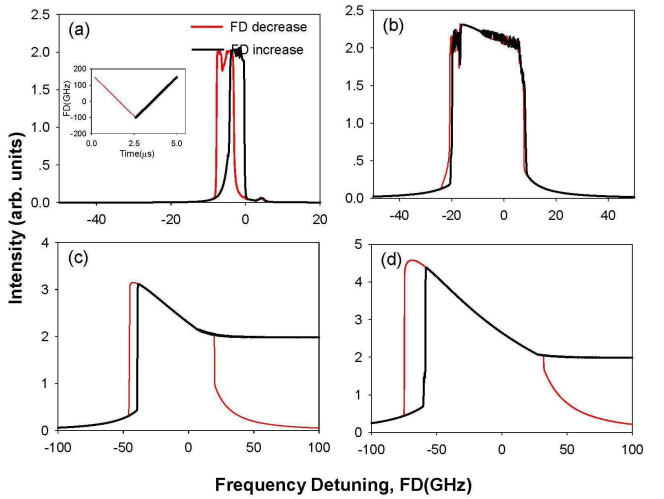

Fig. 5. Polarization behavior under x-injection. For clarity only the intensity of the injected mode (x) is shown. The frequency detuning, FD, first decreases (thin-red line) and then increases (thick-black line) as shown in the inset. The parameters are $E_{inj} = 0.015$ (a), 0.15 (b); 0.5 (c) and 1.0 (d), $\mu = 3$, other parameters are as Fig 1b.

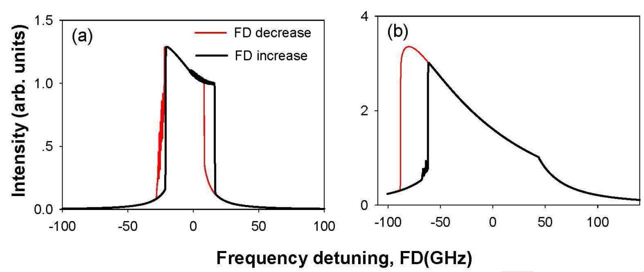

Fig. 6. As Figs. 5b, 5d ($E_{inj} = 0.15$ and 1.0) but with $\mu = 2$.

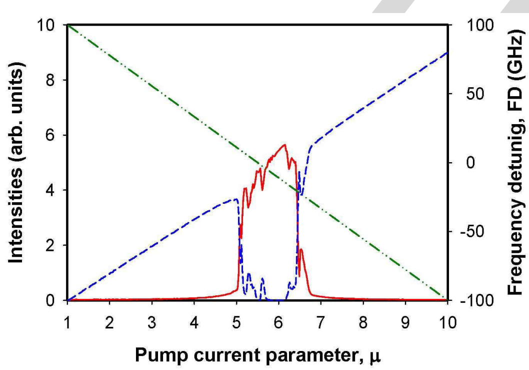

Fig. 7. Polarization-resolved L-I characteristics of the VCSEL with x polarized injection. I_x (solid, red), I_y (dashed, blue). $E_{inj} = 0.2$, other parameters as in Fig. 1b.

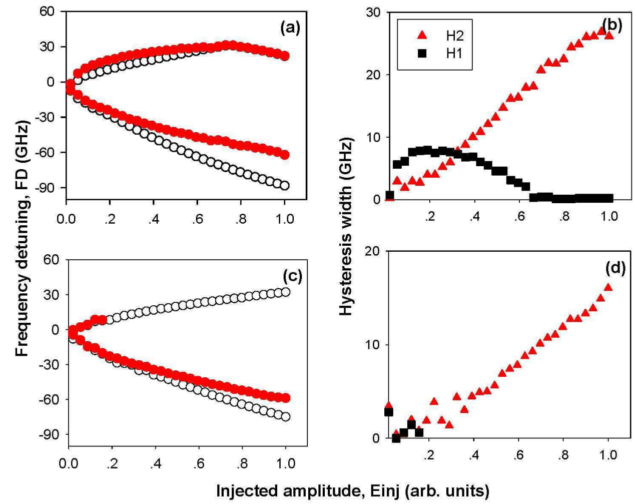

Fig. 8. Polarization switching points when the VCSEL is subjected to x polarized injection (left column, white circles: FD decrease, red circles: FD increase) and width of the hysteresis cycles (right column, H1: black squares, H2: red triangles) vs the amplitude of the injected field, E_{inj}. The pump current parameter is $\mu = 2$ (a,b); $\mu = 3$ (c,d), other parameters as in Fig. 1b.

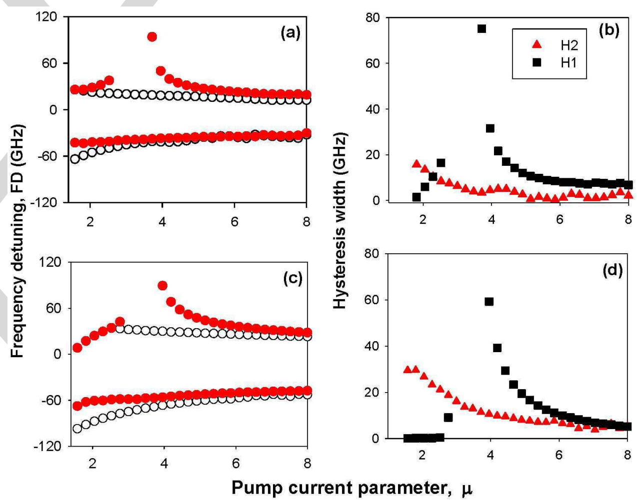

Fig. 9. Polarization switching points when the VCSEL is subjected to x polarized injection (left column, white circles: FD decrease, red circles: FD increase) and width of the hysteresis cycles (right column, H1: black squares, H2: red triangles) vs the bias current parameter, μ. $E_{inj} = 0.5$ (a,b); $E_{inj} = 1.0$ (c,d); other parameters as in Fig. 1b.

weak injection, Fig. 5a, the x polarization turns on in a narrow range of FD values such that the optical frequency of the injected field is close to ω_x, in good agreement with Fig. 3 in [22]. When E_{inj} is increased, an abrupt change in the high-frequency side occurs: due to polarization bistability, the x polarization remains on, even for very large positive detuning values. This is also in good agreement with the observations in Refs. [21] and [22] (see [22, Fig. 4]). We note however that the wide region of bistability in the high frequency side occurs only if the pump current is above a certain value; for lower pump current the two hysteresis cycles remain finite, as seen in Fig. 6.

A wide region of x-polarization emission, induced by the orthogonal injection is seen in the polarization-resolved $L - I$ curve of the injected VCSEL, see Fig. 7. Here the frequency detuning varies with the pump current as indicated with the green line, and the polarization switching are induced by the combined interplay of bias current and detuning variation; if the detuning is kept fixed, there is no switching but a region of polarization coexistence. We remark that the free-running VCSEL emits only the y-polarization, as seen in Fig. 1b. The two polarization switchings shown in Fig. 7 are also in good agreement with the observations in [22] (see [22, Fig. 7]).

Figures 8 and 9 summarize these observations by plotting the FD values when the polarization switchings occurs, and the

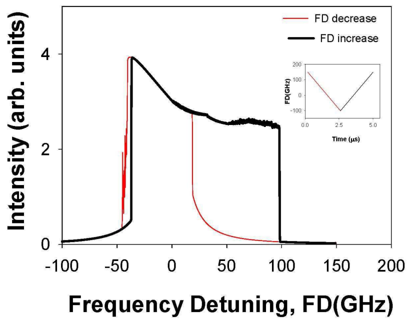

Fig. 10. Wide hysteresis cycle occurring for x polarized injection. $E_{\text{inj}} = 0.5$, $\mu = 3.72$, other parameters as in Fig. 1b.

width of the hysteresis cycles H1 and H2, vs the injected field amplitude (Fig. 8) and vs the pump current (Fig. 9). For parameters such that there is bistability in the high frequency side, there is no hysteresis cycle and H1 is not plotted. We note that the variation of H2 with E_{inj} and μ is similar as that in Figs. 3 and 4 (*i.e.*, H2 increases with E_{inj} and decreases with μ). An example of a very wide H1 hysteresis cycle ($\sim$80 GHz) is presented in Fig. 10.

IV. Conclusions and Discussion

We studied numerically polarization switching and hysteresis phenomena in VCSELs subjected to orthogonal optical injection.

Within the framework of the spin-flip model (SFM) we considered two sets of parameters, representing two situations, one in which the free-running laser emits the high-frequency polarization (mode y in the SFM model) and the injected mode is the x (low-frequency) polarization, and one in which the free-running laser emits the low-frequency polarization (mode x) and the injected mode is the y (high-frequency) polarization. We found that with x-injection the width of the hysteresis cycle in the positive detuning side (H1) can be much wider than that in the negative detuning side (H2), see Figs. 8b, 8d, 9b and 9d and even there is irreversible PS in a wide range of parameters (no switch back occurs).

These results are in good qualitative agreement with recent experimental observations [21], [22] and are interpreted, as in [21] and [22], as due to two-mode stability, either present in the free-running VCSEL for high enough pump current [16], or induced by the external orthogonal injection. On the contrary, with y-injection, we have not found irreversible PS and moreover, we found that H2 >H1 (see Figs. 3b, 3d, 4b and 4d). In this case the linear stability analysis of the free-running VCSEL [16] indicates that at high pump currents there is no bistability but the x and y polarizations are both unstable.

Our results provide a plausible interpretation of why irreversible PS was not observed in [17]–[20] and we hope that they will motivate further experiments to contrast the SFM model predictions regarding the different hysteresis effects induced by x or y polarized injection. In future work it will be interesting to analyze the effect of the birefringence parameter as preliminary simulations suggest that is has a crucial role in the appearance of irreversible polarization switching and ultra-wide hysteresis.

Acknowledgment

The authors would like to thank Professor Alan Shore who shared a preprint of the results published in Refs. [21] and [22].

References

[1] S. Wieczorek, B. Krauskopf, T. B. Simpson, and D. Lenstra, "The dynamical complexity of optically injected semiconductor lasers," *Phys. Rep.*, vol. 416, nos. 1–2, pp. 1–128, 2005.

[2] J. Ohtsubo, *Semiconductor Lasers: Stability, Instability and Chaos*, 2nd ed. Berlin, Germany: Springer-Verlag, 2007.

[3] V. Kovanis, A. Gavrielides, and J. A. C. Gallas, "Labyrinth bifurcations in optically injected diode lasers," *Eur. Phys. J. D*, vol. 58, no. 2, pp. 181–186, 2010.

[4] S. C. Chan, S. K. Hwang, and J. M. Liu, "Radio-over-fiber AM-to-FM upconversion using an optically injected semiconductor laser," *Opt. Lett.*, vol. 31, no. 15, pp. 2254–2256, 2006.

[5] S.-C. Chan, S.-K. Hwang, and J.-M. Liu, "Period-one oscillation for photonic microwave transmission using an optically injected semiconductor laser," *Opt. Exp.*, vol. 15, no. 22, pp. 14921–14935, 2007.

[6] Y.-H. Hung, C.-H. Chu, and S.-K. Hwang, "Optical double-sideband modulation to single-sideband modulation conversion using period-one nonlinear dynamics of semiconductor lasers for radio-over-fiber links," *Opt. Lett.*, vol. 38, no. 9, pp. 1482–1484, 2013.

[7] A. Hurtado, J. Mee, M. Nami, I. D. Henning, M. J. Adams, and L. F. Lester, "Tunable microwave signal generator with an optically-injected 1310 nm QD-DFB laser," *Opt. Exp.*, vol. 21, no. 9, pp. 10772–10778, 2013.

[8] T. B. Simpson, J.-M. Liu, M. AlMulla, N. G. Usechak, and V. Kovanis, "Limit-cycle dynamics with reduced sensitivity to perturbations," *Phys. Rev. Lett.*, vol. 112, no. 2, p. 023901, 2014.

[9] Y. Hong, K. A. Shore, A. Larsson, M. Ghisoni, and J. Halonen, "Pure frequency-polarisation bistability in vertical cavity surface-emitting semiconductor laser subject to optical injection," *Electron. Lett.*, vol. 36, no. 24, pp. 2019–2020, Nov. 2000.

[10] M. Sciamanna and K. Panajotov, "Route to polarization switching induced by optical injection in vertical-cavity surface-emitting lasers," *Phys. Rev. E*, vol. 73, p. 023811, Feb. 2006.

[11] M. Torre, A. Hurtado, A. Quirce, A. Valle, L. Pesquera, and M. Adams, "Polarization switching in long-wavelength VCSELs subject to orthogonal optical injection," *IEEE J. Quantum Electron.*, vol. 47, no. 1, pp. 92–99, Jan. 2011.

[12] J. P. Toomey *et al.*, "Stability of the nonlinear dynamics of an optically injected VCSEL," *Opt. Exp.*, vol. 20, no. 9, pp. 10256–10270, 2012.

[13] C.-H. Chen *et al.*, "All-optical memory based on injection-locking bistability in photonic crystal lasers," *Opt. Exp.*, vol. 19, no. 4, pp. 3387–3395, 2011.

[14] S. Perrone, R. Vilaseca, and C. Masoller, "Stochastic logic gate that exploits noise and polarization bistability in an optically injected VCSEL," *Opt. Exp.*, vol. 20, no. 20, pp. 22692–22699, 2012.

[15] M. F. Salvide, C. Masoller, and M. S. Torre, "All-optical stochastic logic gate based on a VCSEL with tunable optical injection," *IEEE J. Quantum Electron.*, vol. 49, no. 10, pp. 886–893, Oct. 2013.

[16] J. Martín-Regalado, F. Prati, M. S. Miguel, and N. B. Abraham, "Polarization properties of vertical-cavity surface-emitting lasers," *IEEE J. Quantum Electron.*, vol. 33, no. 5, pp. 765–783, May 1997.

[17] I. Gatare, K. Panajotov, and M. Sciamanna, "Frequency-induced polarization bistability in vertical-cavity surface-emitting lasers with orthogonal optical injection," *Phys. Rev. A*, vol. 75, no. 2, p. 023804, 2007.

[18] W. L. Zhang, W. Pan, B. Luo, M. Y. Wang, and X. H. Zou, "Polarization switching and hysteresis of VCSELs with time-varying optical injection," *IEEE J. Sel. Topics Quantum Electron.*, vol. 14, no. 3, pp. 889–894, May/Jun. 2008.

[19] A. Quirce, A. Valle, and L. Pesquera, "Very wide hysteresis cycles in 1550-nm VCSELs subject to orthogonal optical injection," *IEEE Photon. Technol. Lett.*, vol. 21, no. 17, pp. 1193–1195, Sep. 1, 2009.

[20] A. Hurtado, A. Quirce, A. Valle, L. Pesquera, and M. J. Adams, "Power and wavelength polarization bistability with very wide hysteresis cycles in a 1550 nm-VCSEL subject to orthogonal optical injection," *Opt. Exp.*, vol. 17, no. 26, pp. 23637–23642, 2009.

[21] A. A. Qader, Y. Hong, and K. A. Shore, “Robust irreversible polarization switching in optically injected VCSELs,” *IEEE Photon. Technol. Lett.*, vol. 25, no. 12, pp. 1173–1176, Jun. 15, 2013.

[22] A. A. Qader, Y. Hong, and K. A. Shore, “Ultra-wide hysteresis frequency bistability in vertical cavity surface emitting lasers subject to orthogonal optical injection,” *Appl. Phys. Lett.*, vol. 103, no. 2, pp. 021108-1–021108-4, Jul. 2013.

Matias F. Salvide received the M.S.Sc. degree in physics from the Universidad Nacional del Centro de la Provincia de Buenos Aires, Tandil, Argentina, in 2012. He is currently pursuing the Ph.D. degree in physics. His current research interests are in the areas of dynamics of vertical-cavity surface-emitting lasers and optical injection effects in semiconductor lasers.

Cristina Masoller is currently an Associated Professor with the Universitat Politècnica de Catalunya (UPC), Barcelona, Spain. She has more than 20 years of teaching experience at both graduate and postgraduate levels, and co-authored over 120 articles. She received the B.Sc. and M.Sc. degrees in physics from the Universidad de la República (UDELAR), Montevideo, Uruguay, and the Ph.D. degree in physics from Bryn Mawr College, Bryn Mawr, PA, USA, in 1999. From 1992 to 2004, she was an Assistant Professor with UDELAR, and a Ramon i Cajal Researcher with UPC from 2004 to 2009. She was a Visiting Researcher with the University of Nice Sophia Antipolis, Nice, France, in 1999, the Universitat de les Illes Balears, Palma, Spain, from 2001 to 2002, and Bangor University, Bangor, U.K., from 2002 to 2003, and an Associated Researcher with International Centre for Theoretical Physics (ICTP), São Paulo, Brazil, from 2003 to 2006. She is a Program Committee Member of international conferences, including the Conference on Lasers and Electro-Optics/Europe and the International Semiconductor Laser Conference. She has co-organized six workshops on Laser Dynamics and Nonlinear Photonics (Uruguay 2003, 2005, 2007, 2009, 2011, and 2013), and a two-week School on Nonlinear Optics and Nanophotonics for Ph.D. students (ICTP-South American Institute for Fundamental Research, 2013). In 2009, she received the ICREA ACADEMIA Award from Generalitat de Catalunya. Her research interests include optical instabilities and chaos, extreme pulses (optical rogue waves) in semiconductor lasers, synchronization and stochastic phenomena, and high-dimensional dynamics induced by optical feedback. A main research goal has been exploiting stochastic and nonlinear phenomena for novel applications.

Maria Susana Torre received the M.S.Sc. degree in physics and the Ph.D. degree from the Universidad Nacional del Centro de la Provincia de Buenos Aires (UNCPBA), Tandil, Argentina.

She has been a member of the Instituto de Física Arroyo Seco, Tandil, and Centro de Investigaciones en Fisica e Ingenieria del Centro de la Provincia de Buenos Aires, Tandil, since 1988. She is currently a Research Professor with the Facultad de Ciencias Exactas, UNCPBA, and an Independent Researcher with the National Council of Scientific and Technical Investigations, Tandil. Her current research interests include optical switching in vertical cavity surface emitting semiconductor lasers, modeling and dynamics of VCSEL, dynamics of semiconductor lasers with external injection or optical feedback, applications of nonlinear dynamics in semiconductor lasers, and diffusion effects in semiconductor lasers and optical bistability. She is currently working on the modeling of nonlinear properties of semiconductor lasers and their applications to optical communication systems.

Polarization Switching and Hysteresis in Vertical-Cavity Surface-Emitting Lasers Subject to Orthogonal Optical Injection

Matias F. Salvide, Cristina Masoller, and Maria Susana Torre

***Abstract*— We study polarization switching and hysteresis in a vertical-cavity surface-emitting laser (VCSEL) subject to an orthogonal optical injection, such that the polarization of the injected light is perpendicular to that of the free-running VCSEL. We use the framework of the spin-flip model to characterize the polarization state of the VCSEL as a function of the frequency detuning. With appropriated injection conditions, the orthogonal polarization turns on and locks to the injected field. Increasing and decreasing the detuning across the two locking boundaries results either in narrow or wide hysteresis cycles, or even in irreversible switching. These results are in a good agreement with recent experimental observations.**

***Index Terms*— Vertical-cavity surface-emitting lasers (VCSELs), bistability, polarization switching, optical injection, orthogonal injection.**

I. Introduction

OPTICALLY injected semiconductor lasers display a rich variety of nonlinear phenomena, including stable locking, periodic oscillations, excitable and chaotic behavior [1]–[3]. Regular dynamics can have interesting applications, for example, the period-one oscillation can be used to implement frequency-tunable photonic microwave oscillators [4]–[8]. As vertical-cavity surface-emitting lasers (VCSELs) can emit two orthogonal linear polarization modes, orthogonal optical injection (*i.e.*, injecting light with a polarization that is perpendicular to that of the free-running VCSEL) allows for additional phenomena, such as polarization bistability and switching [9]–[12]. Such polarization bistability and switching can be exploited for implementing all-optical memories [13], logic gates [14], [15], etc.

Here we study polarization switching and hysteresis in a VCSEL subject to orthogonal optical injection from a tunable master laser. The VCSEL dynamics is simulated with the spin-flip model (SFM) [16] that takes into account the coupling between two carrier populations (with spin-up and spin-down) and two optical fields with orthogonal polarizations.

We consider as control parameter the frequency detuning (FD), between the master laser and the free-running slave laser. With strong enough injection, if the detuning is within a range of values, FD2 < FD < FD1, the orthogonal polarization turns on and locks to the injected field. Increasing and decreasing FD across the locking boundaries, either FD1 or FD2, while keeping constant the injected power, results in two successive polarization switchings [17]–[22], one when the injected mode turns on, and one when it turns off. These switchings occur at different values of the detuning when the detuning is increased or is decreased, resulting in hysteresis cycles, which have different features in FD1 and FD2.

Our work is motivated by the recent experimental observation of irreversible polarization switching (IPS) [21] and ultra-wide hysteresis [22]. In [21] the orthogonal mode was observed to persist on even when the control parameter – the injected power or the frequency detuning– was reversed (no switch back was observed). As IPS was observed only in the range of bias currents where two modes are supported (*i.e.*, for $I > 2I_{\text{th}}$; for $I < 2I_{\text{th}}$ only the fundamental mode is supported and no IPS was observed), IPS was interpreted as a specific feature of the regime of two-mode operation. In [22] the experiments were also performed in the region of two-mode operation, with bias currents above $2I_{\text{th}}$, and ultra-wide hysteresis (155 GHz) was observed in the positive detuning region (FD1); in contrast, in the negative detuning region (FD2), the hysteresis cycle had a smaller width (few GHz).

Here we analyze the dependence of the hysteresis width of both cycles on the VCSEL parameters and on the orthogonal optical injection conditions. Regarding the VCSEL parameters, to fit the situation in [21] and [22], they are chosen such that the free-running VCSEL emits a stable linear polarization and no polarization switching occurs over the entire operation range. Regarding the injection conditions, we consider two cases, one in which the free-running laser emits the high-frequency polarization (mode y in the SFM model) and the mode that receives optical injection is the low-frequency polarization (mode x), and one in which the free-running laser emits the low-frequency polarization (mode x) and the injected polarization is the high-frequency one (mode y). We find that, with x-injection (as in [21] and [22]), the width

Manuscript received July 17, 2014; revised August 19, 2014; accepted August 21, 2014. M. F. Salvide and M. S. Torre were supported by the National Scientific and Technical Research Council, Argentina, under Grant PIP 114-200801-00163. C. Masoller was supported in part by the European Office of Aerospace Research and Development under Grant FA8655-12-1-2140, in part by the Spanish Ministerio de Ciencia e Innovacion under Grant FIS2012-37655-C02-01, and in part by the ICREA Academia Programme through the Generalitat de Catalunya under Grant 2009 SGR 1168.

M. F. Salvide and M. S. Torre are with the Facultad de Ciencias Exactas, Instituto de Física Arroyo Seco, Tandil 7000, Argentina (e-mail: marita@exa.unicen.edu.ar; msalvide@exa.unicen.edu.ar).

C. Masoller is with the Departament de Fisica i Enginyeria Nuclear, Universitat Politecnica de Catalunya, Terrassa 08222, Spain (e-mail: cristina.masoller@upc.edu).

Color versions of one or more of the figures in this paper are available online at http://ieeexplore.ieee.org.

Digital Object Identifier 10.1109/JQE.2014.2352032

of the FD1 cycle is much wider than that of the FD2 cycle, and even irreversible PS can be observed, in good agreement with [21] and [22]. On the contrary, our simulations indicate that, with y-injection, the width of the FD2 cycle is wider than that in FD1, and no irreversible PS occurs.

This paper is organized as follows. Section II presents the spin-flip model used for describing the VCSEL dynamics under orthogonal optical injection; Sec. III presents the results of the simulations and Sec. IV presents the discussion of the results and the conclusions.

II. Model

We use the well-know spin-flip model of a VCSEL with external optical injection [11]. The equations, written in the frequency reference frame of the injected field are:

$$\frac{dE_x}{dt} = \kappa(1+i\alpha)(NE_x + inE_y - E_x) - i(\gamma_p + \Delta\omega)E_x - \gamma_a E_x + \sqrt{2\beta_{sp}\,\gamma_N N}\;\;\xi_x + \kappa_x\, E_{inj} \tag{1}$$

$$\frac{dE_y}{dt} = \kappa(1+i\alpha)(NE_y - inE_x - E_y) + i(\gamma_p - \Delta\omega)E_y + \gamma_a E_y + \sqrt{2\beta_{sp}\,\gamma_N N}\;\;\xi_y + \kappa_y\, E_{inj} \tag{2}$$

$$\frac{dN}{dt} = -\gamma_N\left[N(1+|E_x|^2+\left|E_y\right|^2)\right] + \gamma_N\mu - i\gamma_N n(E_y E_x^* - E_x E_y^*) \tag{3}$$

$$\frac{dn}{dt} = -\gamma_s n - \gamma_N n(|E_x|^2+\left|E_y\right|^2) - i\gamma_N N(E_y E_x^* - E_x E_y^*). \tag{4}$$

Here E_x and E_y are the two orthogonal linearly polarized slowly varying components of the field and N and n are two carrier variables: N accounts for the total carrier density, while n accounts for the difference between two carrier populations (with spin-up and with spin-down). The model parameters are: κ is the field decay rate, γ_N is the decay rate of N, γ_s is the spin-flip relaxation rate, α is the linewidth enhancement factor, γ_a is the linear dichroism (when γ_a is positive the y polarization has the lower threshold), γ_p is the linear birefringence (when γ_p is positive the x polarization has the lower frequency) and μ is the pump current parameter (normalized such that the solitary threshold is at $\mu = 1$ in the absence of anisotropies). Spontaneous emission noise is taken into account by $\xi_x(t)$ and $\xi_y(t)$ that are uncorrelated complex Gaussian noise terms of zero mean. We define the noise strength parameter as $D = 2\gamma_N\ N\ \beta_{sp}$ with β_{sp} being the spontaneous emission factor. We consider parameters well above threshold and approximate $N \approx 1$ since above threshold the N is clamped to the threshold value.

The optical injection parameters are: $E_{inj}, \kappa_x, \kappa_y$, and $\Delta\omega$. E_{inj} is the injected field amplitude; κ_x and κ_y are used to select which polarization receives optical injection:

i) x polarized injection: $\kappa_x = \kappa$ and $\kappa_y = 0$;

ii) y polarized injection: $\kappa_y = \kappa$ and $\kappa_x = 0$.

$\Delta\omega = \omega_{inj} - \omega_{ref}$ is the detuning of the injected field, defined with respect to a reference angular frequency $\omega_{ref} = (\omega_x + \omega_y)/2$, with ω_x and ω_y being the optical angular frequencies of the x and y polarizations: $\omega_x = -\gamma_p + \gamma_a\alpha$, $\omega_y = \gamma_p - \gamma_a\alpha$ [16]. For easy comparison with Refs. [21] and [22],

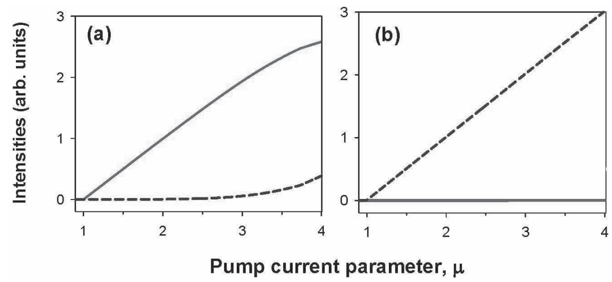

Fig. 1. Polarization-resolved $L-I$ characteristics of the free-running VCSEL. I_x (solid, red), I_y (dashed, blue). (a) $\gamma_p = 60$ rad/ns, $\gamma_a = -0.1$ ns^{-1} and $\gamma_s = 50$ ns^{-1}; (b) $\gamma_p = 10$ rad/ns, $\gamma_a = 1.5$ ns^{-1} and $\gamma_s = 200$ ns^{-1}; other parameters are as indicated in the text.

we define as control parameter the frequency detuning (FD), which is the difference between the frequency of the injected field and that of the free running VCSEL. Therefore,

i) when the free-running laser emits the y polarization, $\mathrm{FD} = (\omega_{\mathrm{inj}} - \omega_{\mathrm{y}})/2\pi$;

ii) when the free-running laser emits the x polarization, $\mathrm{FD} = (\omega_{\mathrm{inj}} - \omega_{\mathrm{x}})/2\pi$.

Also for easy comparison with [22], the width of the hysteresis cycles are defined as

$$\mathrm{H1} = \mathrm{FD}_4 - \mathrm{FD}_3 (\text{high-frequency side})$$

$$\mathrm{H2} = \mathrm{FD}_2 - \mathrm{FD}_{1.} (\text{low-frequency side})$$

where FD_2 and FD_4 (FD_1 and FD_3) are the detuning values for increasing (for decreasing) detuning, when the injected mode turns on and when it turns off.

III. Results

Equations (1)–(4) were simulated with typical VCSEL parameters: $\gamma_N = 1$ ns^{-1}, $\kappa = 300$ ns^{-1}, $\alpha = 3$ and $D = 10^{-5}$ ns^{-1}; for γ_p, γ_a and γ_s we use two sets of values that allow us to consider two situations:

i) For $\gamma_p = 60$ rad/ns, $\gamma_a = -0.1$ ns^{-1} and $\gamma_s = 50$ ns^{-1} the free-running VCSEL emits the lower frequency polarization (x), thus, we consider y polarized optical injection ($\kappa_y = \kappa$, $\kappa_x = 0$).

ii) For $\gamma_p = 10$ rad/ns, $\gamma_a = 1.5$ ns^{-1} and $\gamma_s = 200$ ns^{-1} the free-running VCSEL emits the higher frequency polarization (y), and now the injected light is x polarized ($\kappa_x = \kappa$ and $\kappa_y = 0$). This case corresponds to the VCSELs used in [21] and [22].

For these parameters, as shown in Fig. 1, for the free-running VCSEL no PS occurs for increasing or decreasing pump current (as in [21] and [22]).

A triangular signal was used to increase and decrease the frequency detuning (FD), keeping all other parameters fixed. The total simulation time was long enough to ensure a quasi-static variation of FD (5 μs). The polarization switching points FD_1, FD_2, FD_3 and FD_4 were computed by averaging over 10 stochastic simulations; in each simulation the switching points were detected by averaging the intensities I_x and I_y over a short time interval (1 ns). The initial conditions were such that the scan of the detuning started from an FD value far (to the left or to the right) from the boundary of the region where the orthogonal polarization turns on.

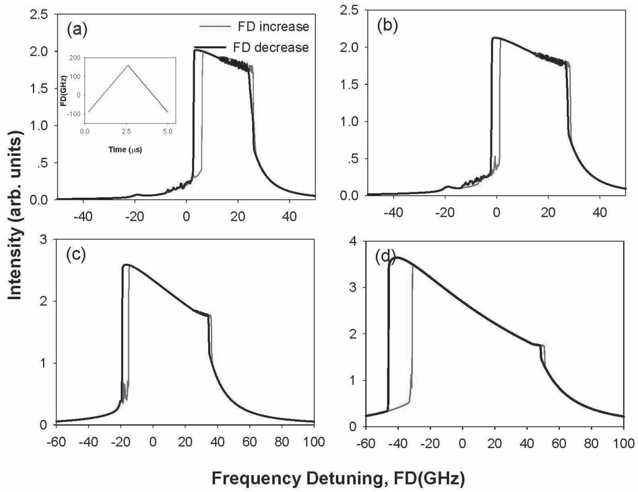

Fig. 2. Polarization behavior under y-injection. For clarity only the intensity of the injected mode (y) is shown, the intensity is averaged over a 1 ns time interval. The frequency detuning, FD, first increases and then decreases, as shown in the inset. $E_{inj} = 0.15$ (a); 0.20 (b); 0.4 (c) and 0.8 (d), $\mu = 2.7$, other parameters are as in Fig. 1a.

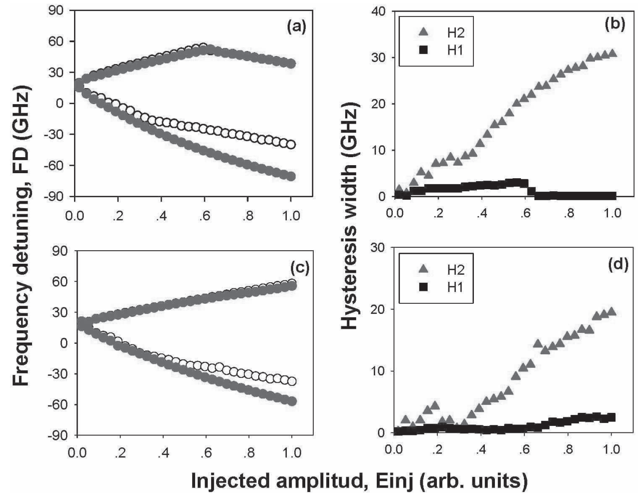

Fig. 3. Polarization switching points when the VCSEL is subjected to y polarized injection (left column, red circles: FD decrease, white circles: FD increase) and width of the hysteresis cycles (right column, H1: black squares, H2: red triangles) vs the amplitude of the injected field, E_{inj}. The pump current parameter is $\mu = 1.8$, (a,b), $\mu = 2.7$ (c, d), other parameters are as Fig 1a.

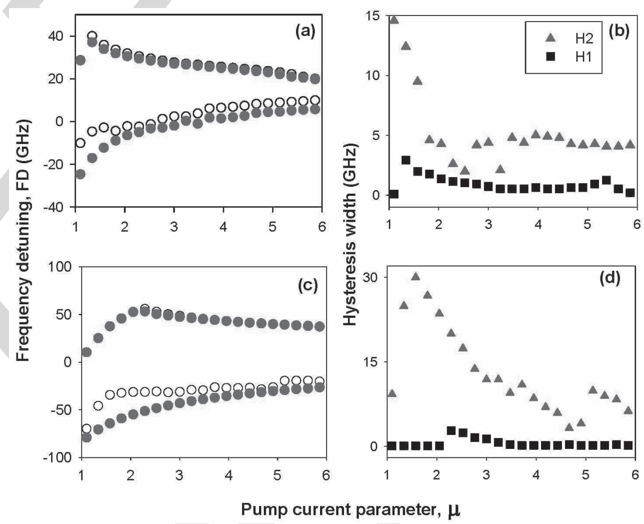

Fig. 4. Polarization switching points when the VCSEL is subjected to y polarized injection (left column, red circles: FD decrease, white circles: FD increase) and width of the hysteresis cycles (right column, H1: black squares, H2: red triangles) vs the bias current parameter, μ. $E_{\text{inj}} = 0.20$ (a,b); 0.8 (c,d); other parameters are as Fig 1a.

Next we present the results of the simulations: first we consider the situation in which the free-running laser emits the x polarization and receives y-polarized injection and then, we consider the situation in which the free-running laser emits the y polarization and receives x-polarized injection.

A. Y Polarized Injection

We consider the first set of parameters, such that the free-running VCSEL emits the x-polarization. We consider orthogonal injection in the y polarization ($\kappa_y = \kappa$, $\kappa_x = 0$). The detuning is defined as $\text{FD} = (\omega_{\text{inj}} - \omega_{\text{x}})/2\pi$.

Figure 2 displays the intensity of the y polarization when the detuning is first increased and then decreased, while the injection strength is kept constant. Simulations for various injection strengths are presented, and it can be observed that the width of the low-frequency side cycle (H2) increases with the injection strength, while the width of the high-frequency side cycle (H1) remains nearly constant.

The left column of Fig. 3 displays the FD values where the y polarization turns on (FD_2 and FD_4) and when it turns off (FD_1 and FD_3) and in the right column, the hysteresis widths (H1 and H2) as a function of the injection strength, for two values of the pump current parameter. With weak optical injection there is polarization competition and the turn-on points of the y polarization are not well defined. This occurs for E_{inj} below 0.05; for stronger injection four switching points define two hysteresis cycles. While the width of the cycle on the high-frequency side, H1, is constant and approximately equal to 3 GHz regardless of the value of E_{inj}, the width of the cycle on the low-frequency side, H2, increases with E_{inj}.

Figure 4 displays the value of the detuning at the four switching points (left column) and the two hysteresis widths (right column) vs the pump current parameter. Simulations for two injection strengths are presented. We observe that for all μ values H1 $<$ H2.

Taken together Figs. 3 and 4 demonstrate that the width of the cycle on the low frequency side (H2) varies with E_{inj} and μ, and large cycles occur for certain parameters ($E_{\text{inj}} \approx 0.8$, $\mu \approx 1.6$). In contrast, the width of the cycle on the high frequency side (H1) is smaller and remains nearly constant when varying E_{inj} or μ.

B. X Polarized Injection

Next we consider the second set of parameters, which correspond to the experimental situation in [21] and [22], such that the free-running laser emits the y polarization and the x polarization receives optical injection ($\kappa_x = \kappa$ and $\kappa_y = 0$). Now the frequency detuning is defined as $\text{FD} = (\omega_{\text{inj}} - \omega_{\text{y}})/2\pi$.

Figure 5 displays intensity of the x polarization when the detuning is varied, while the injection strength is kept constant. Simulations for four injection strengths are presented. For very

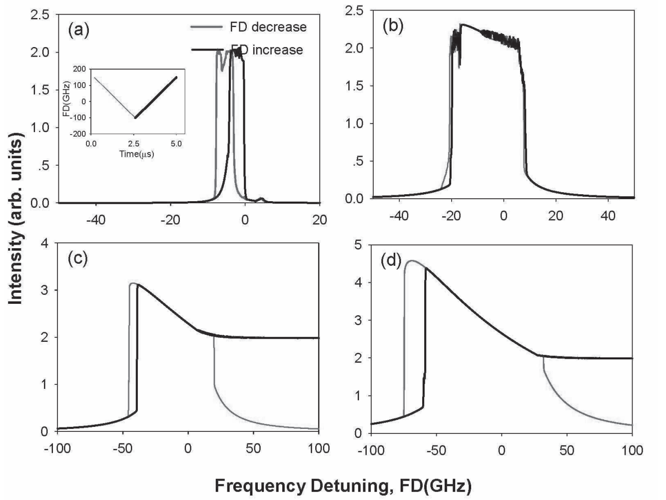

Fig. 5. Polarization behavior under x-injection. For clarity only the intensity of the injected mode (x) is shown. The frequency detuning, FD, first decreases (thin-red line) and then increases (thick-black line) as shown in the inset. The parameters are $E_{inj} = 0.015$ (a), 0.15 (b); 0.5 (c) and 1.0 (d), $\mu = 3$, other parameters are as Fig 1b.

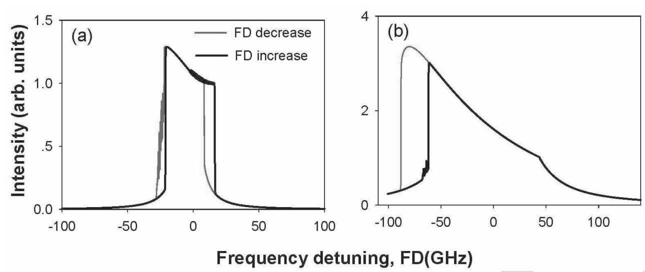

Fig. 6. As Figs. 5b, 5d ($E_{inj} = 0.15$ and 1.0) but with $\mu = 2$.

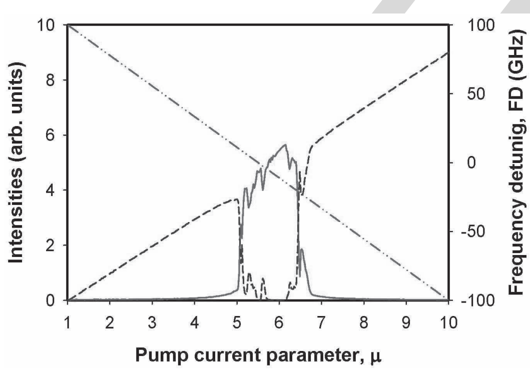

Fig. 7. Polarization-resolved L-I characteristics of the VCSEL with x polarized injection. I_x (solid, red), I_y (dashed, blue). $E_{inj} = 0.2$, other parameters as in Fig. 1b.

weak injection, Fig. 5a, the x polarization turns on in a narrow range of FD values such that the optical frequency of the injected field is close to ω_x, in good agreement with Fig. 3 in [22]. When E_{inj} is increased, an abrupt change in the high-frequency side occurs: due to polarization bistability, the x polarization remains on, even for very large positive detuning values. This is also in good agreement with the observations in Refs. [21] and [22] (see [22, Fig. 4]). We note however that the wide region of bistability in the high frequency side occurs only if the pump current is above a certain value;

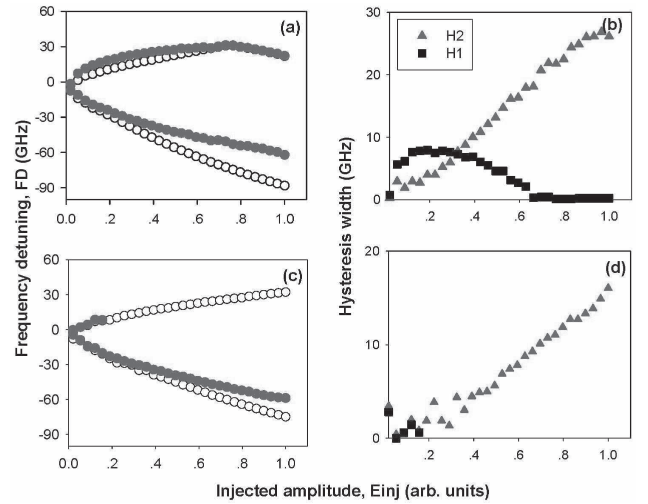

Fig. 8. Polarization switching points when the VCSEL is subjected to x polarized injection (left column, white circles: FD decrease, red circles: FD increase) and width of the hysteresis cycles (right column, H1: black squares, H2: red triangles) vs the amplitude of the injected field, E_{inj}. The pump current parameter is $\mu = 2$ (a,b); $\mu = 3$ (c,d), other parameters as in Fig. 1b.

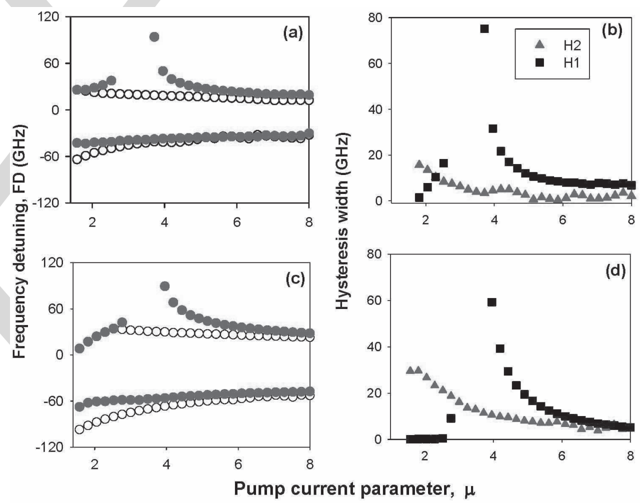

Fig. 9. Polarization switching points when the VCSEL is subjected to x polarized injection (left column, white circles: FD decrease, red circles: FD increase) and width of the hysteresis cycles (right column, H1: black squares, H2: red triangles) vs the bias current parameter, μ. $E_{inj} = 0.5$ (a,b); $E_{inj} = 1.0$ (c,d); other parameters as in Fig. 1b.

for lower pump current the two hysteresis cycles remain finite, as seen in Fig. 6.

A wide region of x-polarization emission, induced by the orthogonal injection is seen in the polarization-resolved $L - I$ curve of the injected VCSEL, see Fig. 7. Here the frequency detuning varies with the pump current as indicated with the green line, and the polarization switching are induced by the combined interplay of bias current and detuning variation; if the detuning is kept fixed, there is no switching but a region of polarization coexistence. We remark that the free-running VCSEL emits only the y-polarization, as seen in Fig. 1b. The two polarization switchings shown in Fig. 7 are also in good agreement with the observations in [22] (see [22, Fig. 7]).

Figures 8 and 9 summarize these observations by plotting the FD values when the polarization switchings occurs, and the

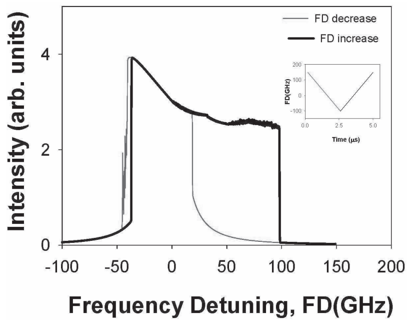

Fig. 10. Wide hysteresis cycle occurring for x polarized injection. $E_{\text{inj}} = 0.5$, $\mu = 3.72$, other parameters as in Fig. 1b.

width of the hysteresis cycles H1 and H2, vs the injected field amplitude (Fig. 8) and vs the pump current (Fig. 9). For parameters such that there is bistability in the high frequency side, there is no hysteresis cycle and H1 is not plotted. We note that the variation of H2 with E_{inj} and μ is similar as that in Figs. 3 and 4 (*i.e.*, H2 increases with E_{inj} and decreases with μ). An example of a very wide H1 hysteresis cycle (∼80 GHz) is presented in Fig. 10.

IV. Conclusions and Discussion

We studied numerically polarization switching and hysteresis phenomena in VCSELs subjected to orthogonal optical injection.

Within the framework of the spin-flip model (SFM) we considered two sets of parameters, representing two situations, one in which the free-running laser emits the high-frequency polarization (mode y in the SFM model) and the injected mode is the x (low-frequency) polarization, and one in which the free-running laser emits the low-frequency polarization (mode x) and the injected mode is the y (high-frequency) polarization. We found that with x-injection the width of the hysteresis cycle in the positive detuning side (H1) can be much wider than that in the negative detuning side (H2), see Figs. 8b, 8d, 9b and 9d and even there is irreversible PS in a wide range of parameters (no switch back occurs).

These results are in good qualitative agreement with recent experimental observations [21], [22] and are interpreted, as in [21] and [22], as due to two-mode stability, either present in the free-running VCSEL for high enough pump current [16], or induced by the external orthogonal injection. On the contrary, with y-injection, we have not found irreversible PS and moreover, we found that H2 >H1 (see Figs. 3b, 3d, 4b and 4d). In this case the linear stability analysis of the free-running VCSEL [16] indicates that at high pump currents there is no bistability but the x and y polarizations are both unstable.

Our results provide a plausible interpretation of why irreversible PS was not observed in [17]–[20] and we hope that they will motivate further experiments to contrast the SFM model predictions regarding the different hysteresis effects induced by x or y polarized injection. In future work it will be interesting to analyze the effect of the birefringence parameter as preliminary simulations suggest that is has a crucial role in the appearance of irreversible polarization switching and ultra-wide hysteresis.

Acknowledgment

The authors would like to thank Professor Alan Shore who shared a preprint of the results published in Refs. [21] and [22].

References

[1] S. Wieczorek, B. Krauskopf, T. B. Simpson, and D. Lenstra, "The dynamical complexity of optically injected semiconductor lasers," *Phys. Rep.*, vol. 416, nos. 1–2, pp. 1–128, 2005.
[2] J. Ohtsubo, *Semiconductor Lasers: Stability, Instability and Chaos*, 2nd ed. Berlin, Germany: Springer-Verlag, 2007.
[3] V. Kovanis, A. Gavrielides, and J. A. C. Gallas, "Labyrinth bifurcations in optically injected diode lasers," *Eur. Phys. J. D*, vol. 58, no. 2, pp. 181–186, 2010.
[4] S. C. Chan, S. K. Hwang, and J. M. Liu, "Radio-over-fiber AM-to-FM upconversion using an optically injected semiconductor laser," *Opt. Lett.*, vol. 31, no. 15, pp. 2254–2256, 2006.
[5] S.-C. Chan, S.-K. Hwang, and J.-M. Liu, "Period-one oscillation for photonic microwave transmission using an optically injected semiconductor laser," *Opt. Exp.*, vol. 15, no. 22, pp. 14921–14935, 2007.
[6] Y.-H. Hung, C.-H. Chu, and S.-K. Hwang, "Optical double-sideband modulation to single-sideband modulation conversion using period-one nonlinear dynamics of semiconductor lasers for radio-over-fiber links," *Opt. Lett.*, vol. 38, no. 9, pp. 1482–1484, 2013.
[7] A. Hurtado, J. Mee, M. Nami, I. D. Henning, M. J. Adams, and L. F. Lester, "Tunable microwave signal generator with an optically-injected 1310 nm QD-DFB laser," *Opt. Exp.*, vol. 21, no. 9, pp. 10772–10778, 2013.
[8] T. B. Simpson, J.-M. Liu, M. AlMulla, N. G. Usechak, and V. Kovanis, "Limit-cycle dynamics with reduced sensitivity to perturbations," *Phys. Rev. Lett.*, vol. 112, no. 2, p. 023901, 2014.
[9] Y. Hong, K. A. Shore, A. Larsson, M. Ghisoni, and J. Halonen, "Pure frequency-polarisation bistability in vertical cavity surface-emitting semiconductor laser subject to optical injection," *Electron. Lett.*, vol. 36, no. 24, pp. 2019–2020, Nov. 2000.
[10] M. Sciamanna and K. Panajotov, "Route to polarization switching induced by optical injection in vertical-cavity surface-emitting lasers," *Phys. Rev. E*, vol. 73, p. 023811, Feb. 2006.
[11] M. Torre, A. Hurtado, A. Quirce, A. Valle, L. Pesquera, and M. Adams, "Polarization switching in long-wavelength VCSELs subject to orthogonal optical injection," *IEEE J. Quantum Electron.*, vol. 47, no. 1, pp. 92–99, Jan. 2011.
[12] J. P. Toomey *et al.*, "Stability of the nonlinear dynamics of an optically injected VCSEL," *Opt. Exp.*, vol. 20, no. 9, pp. 10256–10270, 2012.
[13] C.-H. Chen *et al.*, "All-optical memory based on injection-locking bistability in photonic crystal lasers," *Opt. Exp.*, vol. 19, no. 4, pp. 3387–3395, 2011.
[14] S. Perrone, R. Vilaseca, and C. Masoller, "Stochastic logic gate that exploits noise and polarization bistability in an optically injected VCSEL," *Opt. Exp.*, vol. 20, no. 20, pp. 22692–22699, 2012.
[15] M. F. Salvide, C. Masoller, and M. S. Torre, "All-optical stochastic logic gate based on a VCSEL with tunable optical injection," *IEEE J. Quantum Electron.*, vol. 49, no. 10, pp. 886–893, Oct. 2013.
[16] J. Martín-Regalado, F. Prati, M. S. Miguel, and N. B. Abraham, "Polarization properties of vertical-cavity surface-emitting lasers," *IEEE J. Quantum Electron.*, vol. 33, no. 5, pp. 765–783, May 1997.
[17] I. Gatare, K. Panajotov, and M. Sciamanna, "Frequency-induced polarization bistability in vertical-cavity surface-emitting lasers with orthogonal optical injection," *Phys. Rev. A*, vol. 75, no. 2, p. 023804, 2007.
[18] W. L. Zhang, W. Pan, B. Luo, M. Y. Wang, and X. H. Zou, "Polarization switching and hysteresis of VCSELs with time-varying optical injection," *IEEE J. Sel. Topics Quantum Electron.*, vol. 14, no. 3, pp. 889–894, May/Jun. 2008.
[19] A. Quirce, A. Valle, and L. Pesquera, "Very wide hysteresis cycles in 1550-nm VCSELs subject to orthogonal optical injection," *IEEE Photon. Technol. Lett.*, vol. 21, no. 17, pp. 1193–1195, Sep. 1, 2009.
[20] A. Hurtado, A. Quirce, A. Valle, L. Pesquera, and M. J. Adams, "Power and wavelength polarization bistability with very wide hysteresis cycles in a 1550 nm-VCSEL subject to orthogonal optical injection," *Opt. Exp.*, vol. 17, no. 26, pp. 23637–23642, 2009.

[21] A. A. Qader, Y. Hong, and K. A. Shore, “Robust irreversible polarization switching in optically injected VCSELs,” *IEEE Photon. Technol. Lett.*, vol. 25, no. 12, pp. 1173–1176, Jun. 15, 2013.

[22] A. A. Qader, Y. Hong, and K. A. Shore, “Ultra-wide hysteresis frequency bistability in vertical cavity surface emitting lasers subject to orthogonal optical injection,” *Appl. Phys. Lett.*, vol. 103, no. 2, pp. 021108-1–021108-4, Jul. 2013.

Matias F. Salvide received the M.S.Sc. degree in physics from the Universidad Nacional del Centro de la Provincia de Buenos Aires, Tandil, Argentina, in 2012. He is currently pursuing the Ph.D. degree in physics. His current research interests are in the areas of dynamics of vertical-cavity surface-emitting lasers and optical injection effects in semiconductor lasers.

Cristina Masoller is currently an Associated Professor with the Universitat Politècnica de Catalunya (UPC), Barcelona, Spain. She has more than 20 years of teaching experience at both graduate and postgraduate levels, and co-authored over 120 articles. She received the B.Sc. and M.Sc. degrees in physics from the Universidad de la República (UDELAR), Montevideo, Uruguay, and the Ph.D. degree in physics from Bryn Mawr College, Bryn Mawr, PA, USA, in 1999. From 1992 to 2004, she was an Assistant Professor with UDELAR, and a Ramon i Cajal Researcher with UPC from 2004 to 2009. She was a Visiting Researcher with the University of Nice Sophia Antipolis, Nice, France, in 1999, the Universitat de les Illes Balears, Palma, Spain, from 2001 to 2002, and Bangor University, Bangor, U.K., from 2002 to 2003, and an Associated Researcher with International Centre for Theoretical Physics (ICTP), São Paulo, Brazil, from 2003 to 2006. She is a Program Committee Member of international conferences, including the Conference on Lasers and Electro-Optics/Europe and the International Semiconductor Laser Conference. She has co-organized six workshops on Laser Dynamics and Nonlinear Photonics (Uruguay 2003, 2005, 2007, 2009, 2011, and 2013), and a two-week School on Nonlinear Optics and Nanophotonics for Ph.D. students (ICTP-South American Institute for Fundamental Research, 2013). In 2009, she received the ICREA ACADEMIA Award from Generalitat de Catalunya. Her research interests include optical instabilities and chaos, extreme pulses (optical rogue waves) in semiconductor lasers, synchronization and stochastic phenomena, and high-dimensional dynamics induced by optical feedback. A main research goal has been exploiting stochastic and nonlinear phenomena for novel applications.

Maria Susana Torre received the M.S.Sc. degree in physics and the Ph.D. degree from the Universidad Nacional del Centro de la Provincia de Buenos Aires (UNCPBA), Tandil, Argentina.

She has been a member of the Instituto de Física Arroyo Seco, Tandil, and Centro de Investigaciones en Fisica e Ingenieria del Centro de la Provincia de Buenos Aires, Tandil, since 1988. She is currently a Research Professor with the Facultad de Ciencias Exactas, UNCPBA, and an Independent Researcher with the National Council of Scientific and Technical Investigations, Tandil. Her current research interests include optical switching in vertical cavity surface emitting semiconductor lasers, modeling and dynamics of VCSEL, dynamics of semiconductor lasers with external injection or optical feedback, applications of nonlinear dynamics in semiconductor lasers, and diffusion effects in semiconductor lasers and optical bistability. She is currently working on the modeling of nonlinear properties of semiconductor lasers and their applications to optical communication systems.